Proceedings Australian Geothermal Energy Conferences 2013
Brisbane, Australia, 14-15 November 2013

An approximate solution for the predicting the heat extraction from a closed-loop circulation enhanced geothermal reservoir with dipole wells

Bisheng Wu[1], Xi Zhang[1], Rob Jeffrey[1] and Cameron Huddlestone-Holmes[2]

[1]CSIRO Earth Sciences and Resource Engineering, 71 Normanby Road, Clayton, VIC 3169, Australia

[2]CSIRO Earth Sciences and Resource Engineering, 1 Technology Court, Pullenvale QLD 4069, Australia.

ABSTRACT

This paper investigates the heat extraction from an enhanced geothermal reservoir (EGR) using a closed-loop circulation through one fracture in the reservoir connecting one injection and one production well. Based on the fact that heat conduction is very slow, the one-fracture system serving as both injection and outlet is economically not viable, but represents one fracture in an array of such fractures. In this paper, we will employ a few simplifications to make this complex problem tractable theoretically. Heat exchange between the well and its surrounding formation is assumed to be radial and horizontal. Vertical heat conduction dominates the vicinity of an infinite fractured reservoir and flow-induced heat advection transfers injected cool water to outlet hot water. Mathematically, the closed-loop is divided into three portions, i.e. the injection and production wells and the fracture connecting them, with suitable governing equations for temperature change and connection conditions. Semi-analytical solutions in the Laplace space for each portion are found and the Stehfest method is used to obtain the physical values in the time domain. The results produce useful insights for future geothermal reservoir design. For example, the fluid viscosity does not affect greatly the bottom-hole temperature of the injection well and thus the outlet temperature of the EGR system. The flow rates and the well separation distance are two important factors for outlet temperature. Compared to fully numerical methods, this model is more efficient and can be used as a design and optimization tool.

Keywords: approximate solution, closed-loop circulation, Enhance Geothermal System, dipole wells

1. INTRODUCTION

Geothermal energy has become one the most promising alternatives for energy supplies in the future. First, it has inexhaustible sources from beneath of the earth, such as the heat released from the decay of radioactive elements. In Australia, there is a great deal of heat storage from the hot dry rocks with a temperature of more than 200 ^{o}C at a depth of 5 kms and less (Budd et al. 2008). In addition, compared with the conventional energy resources, such as coal, the geothermal energy has some advantages. For example it is a renewable and clean energy resource. The closed-loop EGR system does not give out any emissions or wastes. Therefore, it is of great importance to study the thermal behavior of an EGR system both experimentally and theoretically for geothermal industrial design, optimization and production assessment.

For an EGR circulation system, we consider three main portions in our analysis. In the injection well, the cold fluid flows downwards and absorbs heat from the surrounding formation at the same time. In the fractured reservoir, the fluid flows towards the production well, and this portion involves the main heat extraction from the reservoir. Then the hot fluid is circulated to the surface through the production well. There have been many studies for each individual portion of this system. For example, as for the fluid flow in the wellbore, Ramey (1962) proposed the fundamental equations for the heat exchange between the fluid flow and the surrounding formation. Later Raymond (1969), Holmes and Swift (1970), Keller et al. (1973), Sump and Williams (1973), Wooley (1980), Fomin et al. (2005), and Wu et al. (2013a) studied similar problems using several different solution approaches, namely finite difference methods and analytical or semi-analytical approaches. For the purpose of simplification, in our work presented below, the effect of the temperature and pressure on the material properties such as the viscosity and mass density are not taken into account.

There are also a great number of studies on the heat extraction from a fracture-like reservoir. For the simple cases where the fluid flow is one-dimensional (for example, radial fluid flow) or the fluid velocity is uniform (for example, flow in the straight crack), the analytical solution is easy to obtain (Lauwerier, 1955; Gringarten, et al. 1975; Cheng et al. 2001; Yang and Yeh 2009). When considering more complex cases, for example an EGR configured with one injection well and one production well, the analytical solutions are difficult to obtain because the problem is 2D or 3D. Gringarten and Sauty (1975) applied successfully the streamline concept to the heat extraction from aquifers with uniform regional flow. By doing this, the fluid flow along a specific streamline can be studied independently, thus reducing the number of dimension by one and simplifying the problem. Following Gringarten and Sauty's idea, Rodemann (1982), Heuer et al. (1991), Schulz (1997), Ogino et al. (1999) and Wu et al. (2013b) utilized the approach of velocity potential and streamline functions (DaCosta and Bennett, 1960; Grove et al. 1970) to study a circular finite or infinite reservoir with dipole or multiple injection and production wells.

Clearly, the well-based solution itself cannot be applied to a closed-loop geothermal system, as the connection conditions are not considered. As for the closed-loop circulation for an EGR with dipole wells, the non-symmetric boundary conditions for injection and production wells add more complexities to obtaining an analytical solution for the temperature evolution. Although numerical methods such as finite element (Kolditz 1995) and boundary element methods (Ghassemi et al. 2003) are able to solve a variety of problems with any boundary and initial conditions, they demand a high computational cost and thus are less suitable for optimization problems.

The aim of this paper is to obtain semi-analytical solutions for the closed-loop EGR in an effective manner as an aid in predicting the output power of the EGR for future design and optimization. As the reservoir extent is much greater than the well separation, it is treated as infinite. Heat exchange between fluid and rock along the wells and the fractured reservoir is considered using different models to capture the main heat sources. Flow-induced heat advection in the fractured reservoir is taken into account.

This paper is organized as follows: in Section 2 and 3, the problem to be studied is mathematically formulated including the closed-loop EGR system description, governing equations, boundary and initial conditions. Their dimensionless forms and a few controlling parameters are derived in Section 4. This is followed by the solution methods in Section 5 and numerical results in Section 6. In the end, some conclusions are presented in Section 7, which are useful for future engineering design of an EGR system.

2. PROBLEM DESCRIPTION AND ASSUMPTIONS

The closed-loop EGR system studied is shown Figure 1(a). The closed-loop circulation system contains two vertical wells, i.e. one for injection (blue) and the other for production (red), which are connected by an infinite horizontal fracture with a constant aperture. The initial temperature of the system is a function of depth, i.e. $T_0 = A_0 z + B_0$, where A_0 is the geothermal gradient and B_0 is the surface ground temperature. It is assumed that initially the fluid and the rock have reached a thermal balance. At time $t>0$, a Newtonian fluid with a constant temperature T_{in} is injected into the system at a constant volumetric rate Q_1 and at the same time a fluid with a flow rate Q_2 is pumped out from the production well.

The geometrical sizes of the wellbore shown in Figure 1(b) and the reservoir are defined as follows: both the wells have the same depth H, the inner radii of the injection and production wells are r_{t1} (diameter $D_1=2r_{t1}$) and r_2 (diameter $D_2=2r_{t2}$), respectively. The aperture of the fracture reservoir is ω. The horizontal distance between the two wells is $2L$ (generally several hundred meters for a commercial EGR). The origin of the general coordinate system is located at the middle point of the line connecting the ground points of the two wells and the vertical axis points downwards.

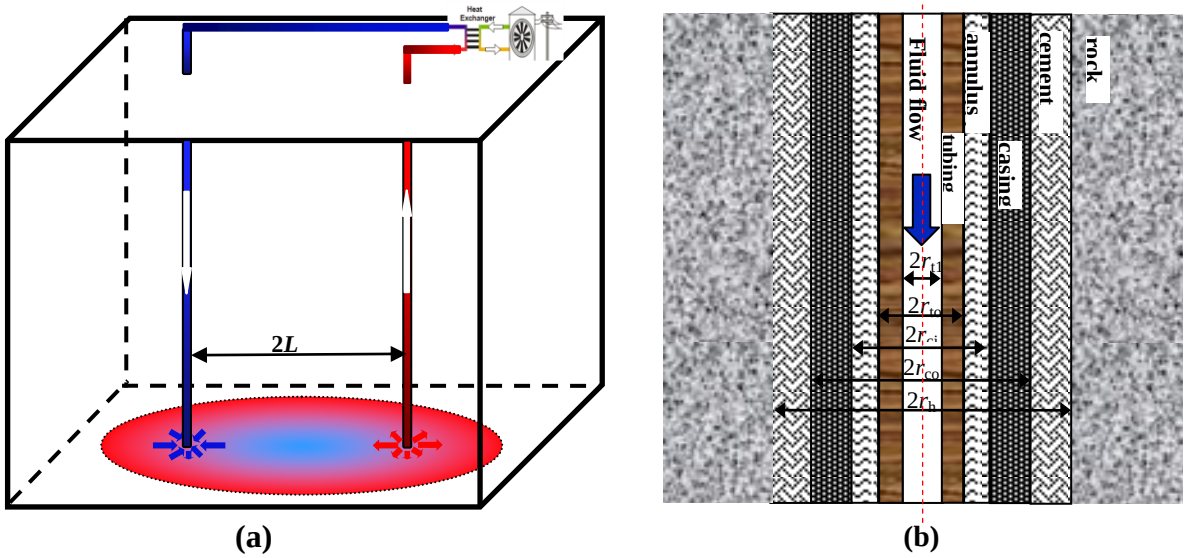

Figure 1: (a) circulation model for a closed-loop EGR and (b) injection well system (for the production well system, the inner radius of the tubing should be replaced with r_{t2} and the fluid flow is upwards).

Some assumptions are made in order to make the problem tractable:

(a) the fluid is single phase, incompressible and Newtonian, and the rock is impermeable. The material properties of the fluid and the rock are constants independent of temperature;

(b) the fluid flow in the fractured reservoir is assumed to reach a steady-state in a short time compared with the long operation life of the reservoir;

(c) the heat flow around the well follows the plane-strain assumption and the heat flow close to the fracture reservoir is modelled using a one-dimensional vertical diffusion equation.

According to JiJi (2009, page 242-246), for a semi-infinite domain with a homogenous initial temperature and one time-dependent surface heat flux $q_0(t)$ imposed at the boundary at $t>0$, the penetration depth of the thermal layer can be obtained by using a heat balance integral method

$$\delta(t) = \left[\frac{6\kappa_r}{q_0(t)} \int_0^t q_0(t) dt \right]^{1/2} \tag{1}$$

where t is the time and $\kappa_r=\lambda_r/(\rho_r c_r)$ is the thermal diffusivity with λ_r, ρ_r and c_r being the thermal conductivity, mass density and specific heat capacity, respectively, of the media.

Take granite for example. When the surface heat flux is a constant, λ_r=2.4W/(m.K), ρ_r=2700Kg/m^3 and c_r=790 J/(Kg.K), $\kappa_r=1.125\times10^{-6}$m^2/s. This means that after 20 years, the thermal layer is about 65.25 m, which is much smaller than the well distance (generally larger than 500 m). This indicates that the well interaction cannot affect significantly the thermal diffusion mode around

each well. In addition, as the plane-strain assumption is adopted, the temperature fields can be described by a radial diffusion equation.

3. GOVERNING EQUATIONS

Based on the above assumptions, the governing equations can be written in the corresponding local coordinate system (LCS) for the injection well, fracture reservoir and production well.

(a) Heat exchange along the wellbore

As the heat flow is assume to be axis-symmetric and horizontal in the region near the wellbore, the energy equations for the fluid flow in the wellbore are written as follows, according to their local cylindrical coordinate system (LCCS)

$$\begin{aligned}
&\rho_f c_f A_1 v_1 \frac{\partial T_{f1}}{\partial z} + 2\pi r_{t1} U_1 (T_{f1} - T_{b1}) = -\rho_f c_f A_1 \frac{\partial T_{f1}}{\partial t}, \ \text{(Injection well)} \\
&h_1 (T_{b1} - T_{f1}) = \lambda_r \frac{\partial T_{r1}}{\partial r}, \quad \text{at } r = r_{t1} \text{ (injection well)} \\
&\rho_f c_f A_2 v_2 \frac{\partial T_{f2}}{\partial z} + 2\pi r_2 U_2 (T_{b2} - T_{f2}) = \rho_f c_f A_2 \frac{\partial T_{f2}}{\partial t}, \text{(Production well)} \\
&h_2 (T_{b2} - T_{f2}) = \lambda_r \frac{\partial T_{r2}}{\partial r^*}, \quad \text{at } r^* = r_2 \text{ (production well)}
\end{aligned} \tag{2}$$

where c_f is the specific heat capacity of the fluid, A_ℓ, h_ℓ, $T_{f\ell}$ and $T_{b\ell}$ (ℓ=1 for injection and ℓ=2 for production) are the areas of the wellbore cross section, overall heat transfer coefficients (HTCs), fluid temperature and the temperature at the wellbore wall, respectively. It should be noted that for the injection well, the origin of the LCCS is at (-L,0,0) with the radial spatial variable r, while for the production well the origin of the LCCS is at (L,0,0) with the radial spatial variable r^* (z positive downwards). The overall HTCs can be calculated based on Willhite's equation (1967)

$$\frac{1}{U_\ell} = \frac{r_{to}}{r_{t\ell} h_\ell} + \frac{r_{to}\ln(r_{to}/r_{t\ell})}{k_{tub.}} + \frac{r_{to}\ln(r_{ins.}/r_{to})}{k_{ins}} + \frac{r_{to}}{r_{ins.}(h_c^{'} + h_r^{'})} + \frac{r_{to}\ln(r_{co}/r_{ci})}{k_{cas.}} + \frac{r_{to}\ln(r_h/r_{co})}{k_{cem.}}, \ (\ell = 1, 2) \tag{3}$$

where the geometrical variables can be found in Figure 1(b). k denotes the thermal conductivity of the corresponding material shown in the subscript. If the effects of the annulus, casing and cements are not taken into account, the first two terms on the right side of Eq.(3) are used to calculate U_ℓ. The variable h_ℓ is the HTC for the fluid flow in the tubing and is obtained by using the relationship $N_u = h\lambda_f / D$, where N_u denotes the Nusselt number, λ_f is the thermal conductivity the fluid and D the hydraulic diameter. For fully developed laminar flow in a pipe with circular cross section, the Nusselt number N_u =3.66, while for transitional and turbulent flows, the Nusselt number is obtained by using the well-known Gnielinski correlation (Gnielinski, 1976)

$$Nu_\ell = \frac{(\xi/8)(\mathrm{Re}_\ell - 1000)\,\mathrm{Pr}_\ell}{1 + 12.7\sqrt{\xi/8}\,(\mathrm{Pr}_\ell^{2/3} - 1)} \left(\frac{\mathrm{Pr}_\ell}{\mathrm{Pr}_r}\right)^{0.11}, \ \xi = \left[0.79\ln(\mathrm{Re}_\ell) - 1.64\right]^{-2}, \tag{4}$$

when $0.5 < \mathrm{Pr}_f < 2000$ and $3000 < \mathrm{Re}_\ell < 5\times10^6$.

(b) Heat conduction in the rock formation surrounding the wellbore

As the radial and horizontal heat conduction dominates the thermal diffusion process around the wellbore, the equations are written as in their corresponding LCCS

$$\frac{\partial T_{r1}}{\partial t} = \kappa_r \frac{1}{r}\frac{\partial}{\partial r}\left(r\frac{\partial T_{r1}}{\partial r}\right), \ \text{(injection well)}; \quad \frac{\partial T_{r2}}{\partial t} = \kappa_r \frac{1}{r^*}\frac{\partial}{\partial r^*}\left(r^*\frac{\partial T_{r2}}{\partial r^*}\right), \text{(production well)} \tag{5}$$

where T_{r1} and T_{r2} denote the temperature of the formation around the injection well and production well, respectively.

(c) Heat conduction for the rock formation between but far from the wellbores

Based on the assumptions, the one-dimensional heat conduction (in the z direction) dominates the thermal diffusion in the region near the fracture and thus is

$$\frac{\partial T_r^\ell}{\partial t} = \kappa_r \frac{\partial^2 T_r^\ell}{\partial z^2} (\ell = 1 \text{for the top layer and } \ell = 2 \text{for the bottom layer}). \tag{6}$$

It should be noted that although the horizontal heat conduction is neglected in the above process, the formation temperature T_r^ℓ is still a function of x and y.

(d) Heat balance at the fractured reservoir

As for the fluid flow in the fracture, the temperature continuity is assumed and the heat balance equation is simplified based on the fact that the conduction in the fluid is trivial and that the convection dominates the heat flow (Cheng et al., 2001)

$$\begin{aligned} &T_r^1 = T_r^2, \qquad \text{on } z = H, \\ &\rho_f c_f \mathbf{q}_f \cdot \nabla T_f + \lambda_r \left(\frac{\partial T_r^1}{\partial z} - \frac{\partial T_r^2}{\partial z} \right) = 0, \text{ on } z = H, \end{aligned} \tag{7}$$

where ∇ and $\nabla\cdot$ are the gradient and divergence operator, respectively. $\mathbf{q}_f$ denotes the discharge vector and can be described by the following equations of Darcy law and mass balance for an incompressible Newtonian fluid in the fracture

$$\mathbf{q}_f = -\nabla \phi_f, \ \nabla \cdot \mathbf{q}_f = Q_1 \delta(x + L, y, H) - Q_2 \delta(x - L, y, H), \tag{8}$$

where ϕ_f denotes the velocity potential for the fluid which is assumed to be steady state and obeys the potential flow theory, δ denotes the Dirac delta function, Q_1 is the injection rate and Q_2 the production rate.

(e) Boundary, connection and initial conditions

The injection rate Q_1 and production rate Q_2 are prescribed. The injection temperature is

$$T_{f1} = T_{in}, \text{ at } (-L, 0, 0). \tag{9}$$

The bottomhole temperature (BHT) of the injection well is assumed to be equal to the fluid temperature flowing into the fracture at that point and the BHT of the production well is assumed to be equal to the fluid temperature flowing out of the fracture, i.e.

$$T_{f1} = T_f, \quad \text{at } (-L, 0, H), \ \ T_{f2} = T_f, \quad \text{at } (L, 0, H). \tag{10}$$

The ground temperature at the surface is a constant

$$T_r^1 = B_0, \quad \text{on } z = 0. \tag{11}$$

The initial temperature of the whole system is a function of depth

$$T_0 = A_0 z + B_0. \tag{12}$$

4. DIMNSIONALESS FORMULATION

The governing equations, boundary and initial conditions are simplified with the following transformation

$$\begin{aligned} &\Theta_{fi} = \frac{T_{f\ell} - B_0}{A_0 H}, \ \Theta_{r\ell} = \frac{T_{r\ell} - B_0}{A_0 H}, \ \Theta_{in} = \frac{T_{in} - B_0}{A_0 H}, \ \Phi_f = \frac{\phi_f - \phi_0}{Q}, \ \Omega_\ell = \frac{Q_\ell}{Q}, \\ &\mathbf{Q}_f = \frac{L}{Q} \mathbf{q}_f, \ R = \frac{r}{r_{t1}}, \ Z = \frac{z}{H}, \ B_\ell = \frac{h_\ell r_{t1}}{\lambda_r}, \ \tau = \frac{\kappa_r t}{r_{t1}^2}, \ X = \frac{x}{L}, \ Y = \frac{y}{L}, \ Z = \frac{z}{L}, \\ &\chi = \frac{\lambda_r L^2}{\rho_w c_w Q H_0}, \chi_\ell = \frac{H \kappa_r}{r_{t1}^2 v_\ell}, \ \alpha_\ell = \frac{2\pi H r_\ell U_\ell}{\rho_f c_f A_\ell v_\ell} = \frac{2\pi H r_\ell U_\ell}{\rho_f c_f Q_\ell}, \ \varepsilon = \frac{r_{t2}}{r_{t1}}, \end{aligned} \tag{13}$$

where ℓ =1 for injection and ℓ =2 for production well.

Heat balance along the wellbore

$$\begin{aligned} &\chi_1 \frac{\partial \Theta_{f1}}{\partial \tau_1} + \frac{\partial \Theta_{f1}}{\partial Z} = \alpha_1 (\Theta_{b1} - \Theta_{f1}), \qquad \text{(injection well)} \\ &B_1 (\Theta_{b1} - \Theta_{f1}) = \frac{\partial \Theta_{r1}}{\partial R}, \qquad \text{at } R = 1, \ \text{(injection well)} \\ &\chi_2 \frac{\partial \Theta_{f2}}{\partial \tau} - \frac{\partial \Theta_{f2}}{\partial Z} = -\alpha_2 (\Theta_{f2} - \Theta_{b2}), \ \text{(production well)} \\ &B_2 (\Theta_{b2} - \Theta_{f2}) = \frac{\partial \Theta_{r2}}{\partial R}, \qquad \text{at } R = \varepsilon. \ \text{(production well)} \end{aligned} \tag{14}$$

Heat conduction in the local region around the wellbore

$$\frac{\partial \Theta_{r1}}{\partial \tau} = \frac{1}{R} \frac{\partial}{\partial R} \left(R \frac{\partial \Theta_{r1}}{\partial R} \right), \ \text{(injection well)}; \ \ \frac{\partial \Theta_{r2}}{\partial \tau} = \frac{1}{R} \frac{\partial}{\partial R} \left(R \frac{\partial \Theta_{r2}}{\partial R} \right) \ \text{(production well)}. \tag{15}$$

Vertical conduction between the wellbore and close to the fracture

$$\frac{\partial \Theta_r^{\ell}}{\partial \tau} = c^2 \frac{\partial^2 \Theta_r^{\ell}}{\partial Z^2},\ c = \frac{r_{t1}}{H}\ (\ell = 1 \text{for top layer and } \ell = 2 \text{for bottom layer}). \tag{16}$$

Temperature and heat flux at the fractured reservoir

$$\Theta_r^1 = \Theta_r^2, \quad \mathbf{Q}_f \cdot \nabla \Theta_f + \chi \left(\frac{\partial \Theta_r^1}{\partial Z} - \frac{\partial \Theta_r^2}{\partial Z} \right) = 0, \text{ on } Z = 1. \tag{17}$$

Fluid flow in the reservoir

$$\mathbf{Q}_f = -\nabla \Phi_f,\ \nabla \cdot \mathbf{Q}_f = \Omega_1 \delta(X+1, Y, 1) - \Omega_2 \delta(X-1, Y, 1). \tag{18}$$

Initial and boundary conditions

$$\begin{aligned} &\Theta_{f1} = \Theta_{in}, \text{ at } (-1,0,0), \\ &\Theta_{f1} = \Theta_f, \quad \text{at } (-1,0,1), \quad \Theta_{f2} = \Theta_f, \quad \text{at } (1,0,1), \\ &\Theta_r^1 = 0, \quad \text{on } Z = 0, \\ &\Theta_0 = Z, \quad \text{on } \tau = 0. \end{aligned} \tag{19}$$

5. SOLUTIONS

As mentioned in the previous sections, the whole closed-loop circulation is divided into three portions: the flow in the injection well, the flow in the fracture reservoir and the flow in the production well. The output temperature in the previous part is regarded as the input condition for the next one. This greatly simplifies the original problem. By using the Laplace transformation, the analytical solutions for the three stages are obtained. In the following equations, the symbol ^ denotes the variables which are Laplace transformed and *s* is the Laplace symbol.

Injection well

Base on Eqns. (14), (15) and (19), the solutions are obtained to be

$$\begin{aligned} &\hat{\Theta}_{r1} = \left\{ \frac{[W(s)s\beta_1 + \Delta_1]}{s\Delta_1\beta_1} e^{-\frac{\beta_1}{\Delta_1}Z} - \frac{1}{s\beta_1} \right\} K_0(\sqrt{s}R_1) + \frac{Z}{s}, \quad \hat{\Theta}_{b1} = \left\{ \frac{[W(s)s\beta_1 + \Delta_1]}{s\Delta_1\beta_1} e^{-\frac{\beta_1}{\Delta_1}Z} - \frac{1}{s\beta_1} \right\} K_0(\sqrt{s}) + \frac{Z}{s}, \\ &\hat{\Theta}_{f1} = \left\{ \frac{[W(s)s\beta_1 + \Delta_1]}{s\Delta_1\beta_1} e^{-\frac{\beta_1}{\Delta_1}Z} - \frac{1}{s\beta_1} \right\} \Delta_1 + \frac{Z}{s}, \quad \Delta_1 = \frac{K_1(\sqrt{s})\sqrt{s}}{B_1} + K_0(\sqrt{s}), \quad \beta_1 = \chi_1 s\Delta_1 + \frac{\alpha_1}{B_1} K_1(\sqrt{s})\sqrt{s}, \end{aligned} \tag{20}$$

where $W(s)$ is the Laplace transform of the injection temperature. K_0 and K_1 are the modified Bessel functions of the second kind. The Laplace transformation of the BHT of the injection well is

$$\hat{\Theta}_{f1,\text{out}} = H(s) = \left(W(s) + \frac{\Delta_1}{s\beta_1} \right) e^{-\frac{\beta_1}{\Delta_1}} - \frac{\Delta_1}{s\beta_1} + \frac{1}{s}. \tag{21}$$

Fracture reservoir

For the purpose of simplicity, assume $Q_1 = Q_2 = Q$, i.e. $\Omega_1 = \Omega_2 = 1$. By using the same approach of velocity potential and streamline functions as Schulz (1997) and Wu et al. (2013), the second equation of (17) is transformed into

$$-V^2 \frac{\partial \Theta_f}{\partial \Phi} + \chi \left(\frac{\partial \Theta_r^1}{\partial Z} - \frac{\partial \Theta_r^2}{\partial Z} \right) = 0,\ V^2 = q_X^2 + q_Y^2, \text{ on } Z = 1, \tag{22}$$

where the components of the discharge vectors q_X and q_Y are

$$\begin{aligned} &q_X = -\frac{\partial \Phi}{\partial X}, \quad \frac{\Phi}{c} = \eta = \frac{1}{2} \ln \left[\frac{(X-1)^2 + Y^2}{(X+1)^2 + Y^2} \right],\ c = \frac{1}{2\pi} \\ &q_Y = -\frac{\partial \Phi}{\partial Y}, \quad \frac{\Psi}{c} = \varsigma = -\arctan \frac{2Y}{1 - X^2 - Y^2}. \end{aligned} \tag{23}$$

From Eq.(23), *X* and *Y* are expressed as in terms of η and ς

$$Y = \frac{\cot \varsigma \pm \cosh \eta \sqrt{\cot^2 \varsigma + 1)}}{(\cot^2 \varsigma \sinh^2 \eta + \cosh^2 \eta)}, \quad X = -(1 + Y \cot \varsigma) \tanh \eta. \tag{24}$$

As the fluid flow is symmetric with respective to *x* axis and the half plane above *x* axis is chosen, then

$$Y=\frac{\cot\varsigma+\cosh\eta\sqrt{\cot^2\varsigma+1)}}{(\cot^2\varsigma\sinh^2\eta+\cosh^2\eta)},\quad X=-(1+Y\cot\varsigma)\tanh\eta, \tag{25}$$

which is also simplified

$$\begin{aligned} Y&=-\frac{\sin\varsigma}{\cos\varsigma+\cosh\eta},\quad X=-\frac{\sinh\eta}{\cos\varsigma+\cosh\eta},\quad \text{when } \varsigma\in\left[-\frac{\pi}{2},0^-\right],\\ Y&=-\frac{\sin\varsigma}{\cos\varsigma-\cosh\eta},\quad X=-\frac{\sinh\eta}{\cosh\eta-\cos\varsigma},\quad \text{when } \varsigma\in\left[0^+,\frac{\pi}{2}\right]. \end{aligned} \tag{26}$$

Equation (16) is solved to be

$$\Theta_r^1=F_1\exp\left(\sqrt{s}/cZ\right)+F_2\exp\left(-\sqrt{s}/cZ\right)+\frac{Z}{s},\ \ \Theta_r^2=F_3\exp\left(\sqrt{s}/cZ\right)+F_4\exp\left(-\sqrt{s}/cZ\right)+\frac{Z}{s}, \tag{27}$$

where F_1, F_2, F_3 and F_4 are unknown functions of Φ, Ψ and s. By using the boundary conditions at Z=0, Z=1 and $Z\rightarrow$ infinity, we obtain F_2=- F_1, F_4=[exp(2/$c\sqrt{}$s)-1] F_1 and F_3=0. Therefore,

$$\Theta_r^1=F_1\left[\exp\left(\sqrt{s}/cZ\right)-\exp\left(-\sqrt{s}/cZ\right)\right]+\frac{Z}{s},\ \ \Theta_r^2=F_1\left[\exp\left(2\sqrt{s}/c\right)-1\right]\exp\left(-\sqrt{s}/cZ\right)+\frac{Z}{s}. \tag{28}$$

Substitution of the above equation into Eq. (22) leads to one ordinary differential equation (ODE) whose solution is found to be

$$F_1=F_5\exp\left(-\frac{2\chi\sqrt{s}/c}{1-\exp\left(-2\sqrt{s}/c\right)}\int_\Phi^{+\infty}\frac{1}{\mathrm{V}^2}d\xi\right), \tag{29}$$

where F_5 is an unknown function of Ψ and s. By using the boundary condition at the injection point of the fracture, F_5 is found to be

$$F_5=\frac{H(s)}{\exp\left(\sqrt{s}/c\right)-\exp\left(-\sqrt{s}/c\right)}. \tag{30}$$

Therefore, the solutions for the temperatures of the rock formation and the fluid in the fracture are

$$\begin{aligned} \hat{\Theta}_r^1&=\exp\left(-\frac{2\chi\sqrt{s}/c}{1-\exp\left(-2\sqrt{s}/c\right)}\int_\Phi^{+\infty}\frac{1}{\mathrm{V}^2}d\xi\right)\frac{\exp\left(\sqrt{s}/cZ\right)-\exp\left(-\sqrt{s}/cZ\right)}{\exp\left(\sqrt{s}/c\right)-\exp\left(-\sqrt{s}/c\right)}\frac{sH(s)-1}{s}+\frac{Z}{s},\\ \Theta_r^2&=\exp\left(-\frac{2\chi\sqrt{s}/c}{1-\exp\left(-2\sqrt{s}/c\right)}\int_\Phi^{+\infty}\frac{1}{\mathrm{V}^2}d\xi\right)\exp\left[-\sqrt{s}/c(Z-1)\right]\frac{sH(s)-1}{s}+\frac{Z}{s},\\ \hat{\Theta}_f&=\exp\left(-\frac{2\chi\sqrt{s}/c}{1-\exp\left(-2\sqrt{s}/c\right)}\int_\Phi^{+\infty}\frac{1}{\mathrm{V}^2}d\xi\right)\frac{sH(s)-1}{s}+\frac{1}{s}. \end{aligned} \tag{31}$$

From Eqns (22), (23) and (26) the integral in the above equation is expressed as

$$\mathrm{g}(\eta,\varsigma)=\int_\Phi^{+\infty}\frac{1}{\mathrm{V}^2}d\xi=\begin{cases}\dfrac{1}{c}\displaystyle\int_\eta^\infty\frac{1}{\left[\cosh\xi+\cos\varsigma\right]^2}d\xi, & \text{when } \varsigma\in\left[-\dfrac{\pi}{2},0^-\right],\\ \dfrac{1}{c}\displaystyle\int_\eta^\infty\frac{1}{\left[\cosh\xi-\cos\varsigma\right]^2}d\xi, & \text{when } \varsigma\in\left[0^+,\dfrac{\pi}{2}\right],\end{cases} \tag{32}$$

where 0^- and 0^+ corresponds to the streamlines along positive and negative axis, respectively. The value of $g(\eta,\varsigma)$ can be obtained based on the formula (2.445) and (2.446) in the book by Gradshteyn and Ryzhik (2007). Here only the results are given

$$\mathrm{g}(\eta,\varsigma)=\begin{cases}\dfrac{1}{c\sin^2\varsigma}\left[1-\dfrac{\sinh\eta}{(\cosh\eta+\cos\varsigma)}-2\cot\varsigma\left\{\arctan\left(\tan\dfrac{\varsigma}{2}\right)-\arctan\left(\tanh\dfrac{\eta}{2}\tan\dfrac{\varsigma}{2}\right)\right\}\right], & \text{when } |\cos\varsigma|\neq 1,\\ \dfrac{1}{3c}\left\{1-\dfrac{\sinh\eta}{\cosh\eta+\cos\varsigma}\left[1+\dfrac{\cos\varsigma}{\cosh\eta+\cos\varsigma}\right]\right\}, & \text{when } |\cos\varsigma|=1.\end{cases} \tag{33}$$

Production well

Based on Eqns. (14) and (15), the solutions for the temperature of the fluid and rock formation wall are obtained

$$\hat{\Theta}_{r2}=\left\{\frac{\left[G(s)\mathrm{s}\,\beta_2-\Delta_2-\beta_2\right]}{s\Delta_2\beta_2}\mathrm{e}^{-\frac{\beta_2}{\Delta_2}(1-Z)}+\frac{1}{s\beta_2}\right\}\mathrm{K}_0\left(\sqrt{s}R_2\right)+\frac{Z}{s},$$
$$\hat{\Theta}_{b2}=\left\{\frac{\left[G(s)\mathrm{s}\,\beta_2-\Delta_2-\beta_2\right]}{s\Delta_2\beta_2}\mathrm{e}^{-\frac{\beta_2}{\Delta_2}(1-Z)}+\frac{1}{s\beta_2}\right\}\mathrm{K}_0\left(\sqrt{s}\right)+\frac{Z}{s},\qquad(34)$$
$$\hat{\Theta}_{f2}=\left\{\frac{\left[G(s)\mathrm{s}\,\beta_2-\Delta_2-\beta_2\right]}{s\Delta_2\beta_2}\mathrm{e}^{-\frac{\beta_2}{\Delta_2}(1-Z)}+\frac{1}{s\beta_2}\right\}\Delta_2+\frac{Z}{s},$$
$$\Delta_2=\frac{\mathrm{K}_1\left(\sqrt{s}\varepsilon\right)\sqrt{s}}{B_2}+\mathrm{K}_0\left(\sqrt{s}\varepsilon\right),\quad \beta_2=\chi_2 s\Delta_2+\frac{\alpha_2}{B_2}\mathrm{K}_1\left(\sqrt{s}\varepsilon\right)\sqrt{s},$$

where G(s) is the Laplace transformation of BHT of the production well, which is obtained from Eq. (31).

6. RESULTS

As used in previous studies, the Stehfest method (1970) is utilized to obtain the values of the solutions in the time space. In this section, the attention is paid to the effect of the fluid viscosity, flow rates and well distance on the temperature evolution in the fluid and the rock formation. Water and granite are chosen as the fluid and reservoir rock, respectively, for the following calculations. The parameters used for the examples are listed in the Table 1 unless otherwise specified.

Parameter	Value	Parameter	Value
Inner radius, injection tubing r_{t1} (m)	0.1	Rock thermal conductivity (W/(m•K)	2.4
Inner radius, production tubing r_{t1} (m)	0.1	Rock specific heat (J/(Kg•K)	790
Outer radius, tubing r_{to} (m)	0.12	Rock density (Kg/(m^3)	2700
Well distance 2L (m)	500	Fluid thermal conductivity (W/(m•K)	0.6
Well depth H_0 (m)	4500	Fluid specific heat (J/(Kg•K)	4200
Fracture aperture (m)	0.001	Fluid density (Kg/(m^3)	1000
Initial pressure (MPa)	75	Fluid viscosity (Pa•s)	5×10^{-4}
Geothermal gradient A_0 (K/m)	0.04	Injection rate Q_1 (m^3/s)	0.020
Surface temperature B_0 (^{o}C)	27	Production rate Q_2 (m^3/s)	0.020

Table 1: physical parameters for the present calculation.

Q_1 (m^3/s)	μ (Pa•s)	v_1 (m/s)	Re_1	h_1 (W/m^2/K)	U_1 (W/m^2/K)	Nu_1	α_1	B_1	χ_1
0.005	5×10^{-4}	0.159	6.37×10^4	100	80.6	301	10.90	4.18	3.180
0.020	5×10^{-4}	0.637	2.55×10^5	335	249	1010	8.39	14.0	0.795
0.030	5×10^{-4}	0.955	3.82×10^5	478	340	1.30	7.62	19.9	0.530
0.050	5×10^{-4}	1.590	6.37×10^5	749	490	2250	6.60	31.2	0.318
0.020	10^{-4}	0.637	1.27×10^6	461	329	1380	11.1	19.2	0.795
0.020	10^{-3}	0.637	1.27×10^5	262	199	785	6.70	10.9	0.795

Table 2: dimensionless parameters under different flow rates and fluid viscosity.

(a) Thermal responses in the injection well

Figure 2 displays the fluid temperature variations with time along the injection well when the flow rate is Q_1=Q_2=0.02m^3/s. The injection temperature T_{in}= 20 ^{o}C and the surface temperature B_0=27 ^{o}C corresponding to a minimum dimensionless value Θ_{in} =-0.038 and Θ_0=0 in terms of the depth as Z. The left-most point and the one where Θ_{f1}=0 on the x-axis in the figure correspond to the injection temperature and the surface temperature, respectively. It can be seen that the fluid temperature along the well decreases rapidly during the first day and approaches the injection temperature after 10 days. After around three months, the fluid temperature at any point along the well is very close to the injection temperature. This means that the injection temperature is the same as the BHT of the injection well, which is taken as the inlet temperature for the fractured reservoir. In this case, the fluid velocity is v_1=0.64 m/s and it takes about 1.95 hours for the fluid to reach the bottom of the well. Although the fluid absorbs heat from the surrounding formation when flowing downwards, the rock around the wellbore is continually cooled and eventually the amount of heat absorbed by the fluid becomes negligible.

The effect of the viscosity on the BHT of the injection well is shown in Figure 3. The water viscosity ranges from about 2.8×10^{-4} Pa•s to 1.3×10^{-3} Pa•s when the temperature changes from 100 ^{o}C to 10 ^{o}C, which can be found in the website link (http://en.wikipedia.org/wiki/viscosity). Here μ =10^{-4}, 5×10^{-4} and 10^{-3} Pa•s are chosen for the water. From Figure 3 the BHT follows exactly the same curve under these three cases. This means that the more/less heat absorbed/released by varying the fluid viscosity and thus by changing the heat transfer coefficients (as shown in Table 2) has little effect on the fluid temperature variations.

In Figure 4, the effect of the injection rates on the BHT of the injection well is displayed. The BHT differences under small and large flow rates is obvious, but becomes smaller and smaller with time increasing. When the flow rate is larger than 0.015 m^3/s, the BHTs follow almost the same trend when the time is long enough. The larger flow rates, the shorter time for the BHT of the injection well to approach the injection fluid temperature.

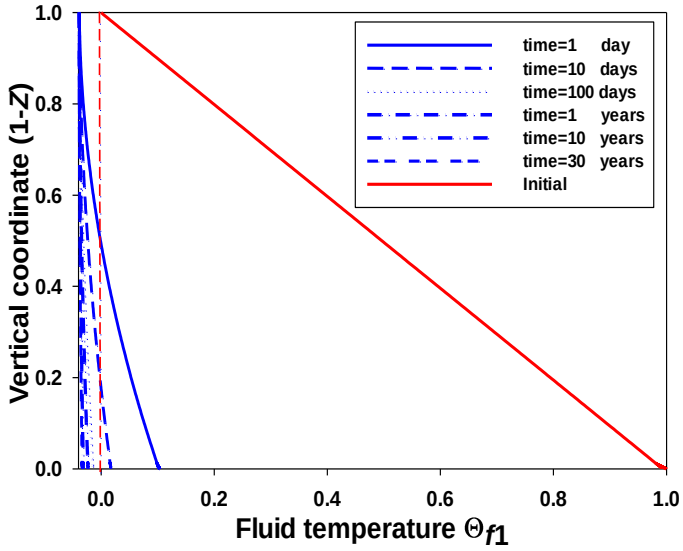

Figure 2: Fluid temperature varying with time along the injection well when $Q_1=Q_2=0.02$ m^3, $\mu=5\times10^{-4}$ Pa•s and $2L=500$ m.

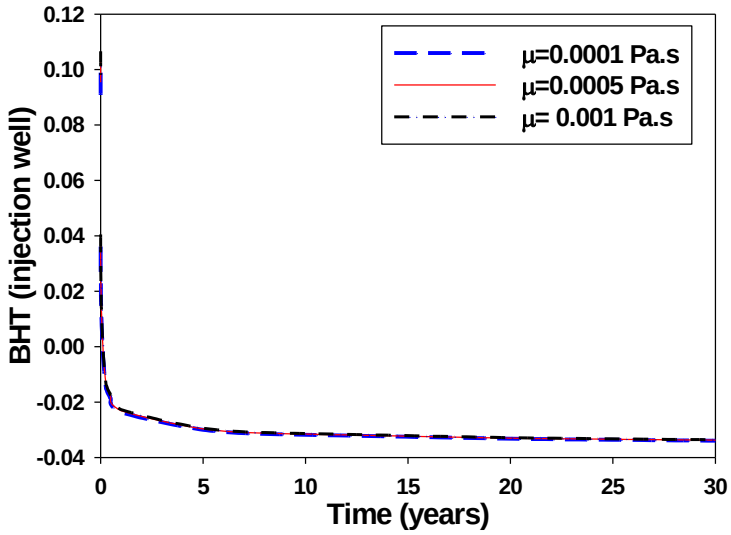

Figure 3: Dimensionless BHT of the injection well as a function of fluid viscosity when $Q_1=Q_2=0.02$ m^3 and $2L=500$ m.

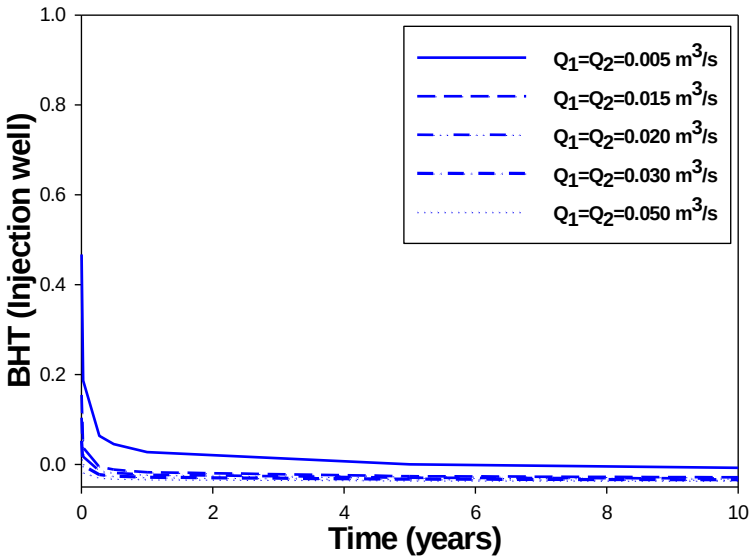

Figure 4: Dimensionless BHT of the injection well under different flow rates when μ=5×10^{-4} Pa•s and 2L=500 m.

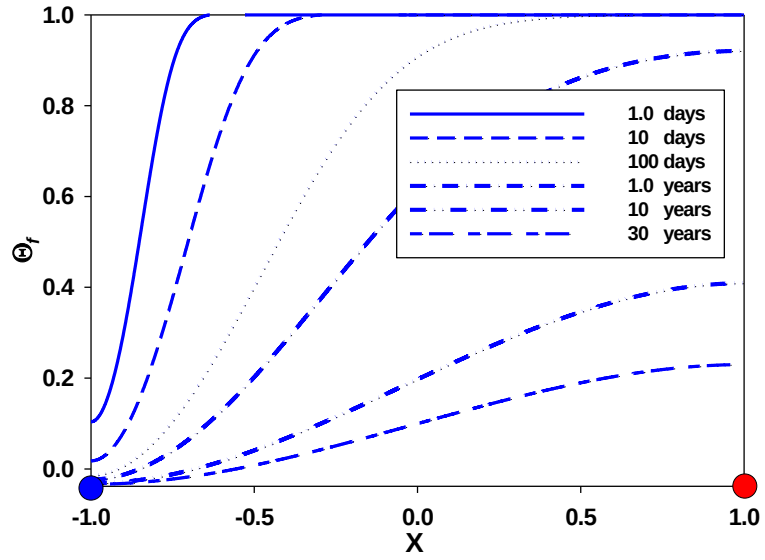

Figure 5: Dimensionless temperature evolution along the line connecting the dipole wells when Q_1=Q_2=0.02 m^3, μ=5×10^{-4} Pa•s and 2L=500 m. The blue circle denotes the injection well and the red one denotes the production well.

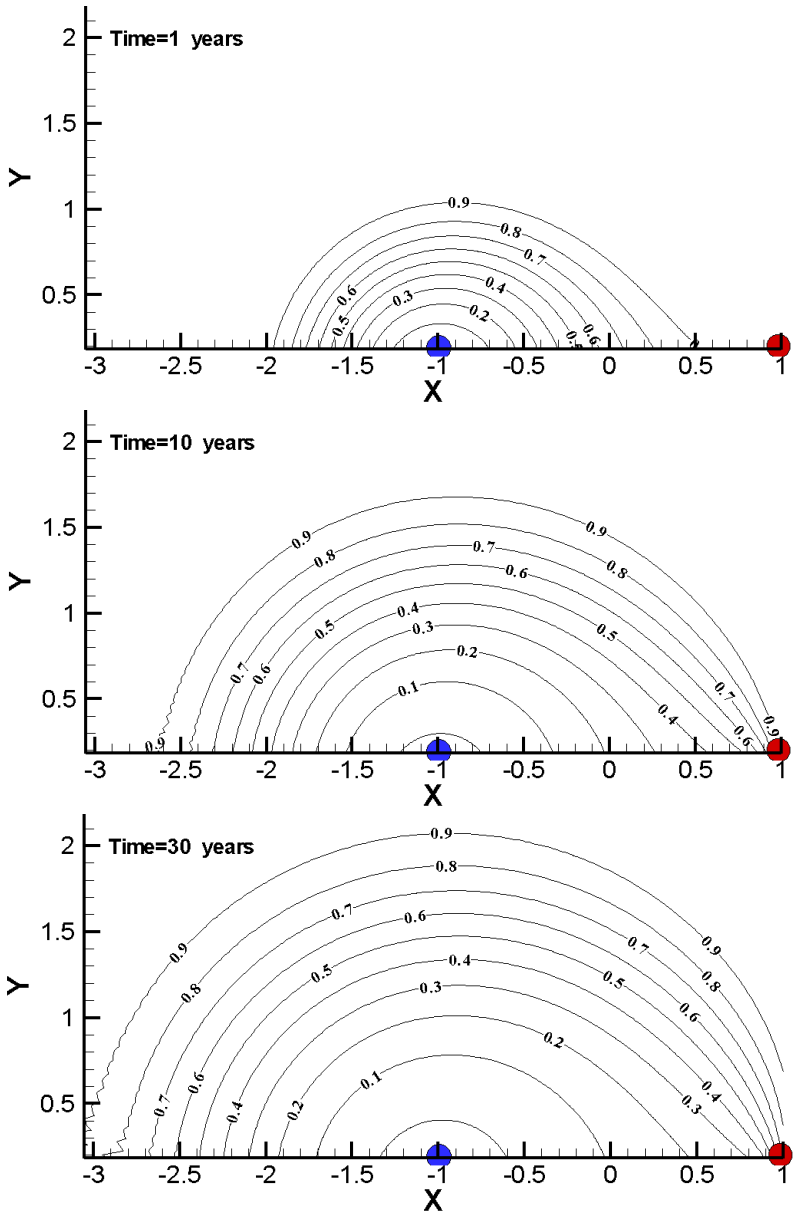

Figure 6: Dimensionless fluid temperature varying with time around the injection well when Q_1=Q_2=0.02 m^3, μ=5×10^{-4} Pa•s and 2L=500 m. The blue circle denotes the injection and the red one production well.

(b) Thermal responses related to the fracture

As the streamlines starting from the injection well run into the production well or approach infinity, the temperature field for the fluid can be obtained by considering each point along the streamline. The streamline trajectory can affect the temperature due to the different exposed time to the hot rocks, and therefore, the BHT in the vicinity of the production well depends on the orientation of the fluid velocity vector approaching the production well. In the current calculation, the BHT of the production well is assumed to be equal to the average temperature of all the points on a small circle centered at the production well, which is taken as the starting temperature for the production well part of the calculation.

Figure 5 shows the temperature evolution along a typical streamline which directly connects the injection and production wells. After small time t=1 day, there is a steep change of temperature near the injection well because of the cold water flowing into the fracture. With increasing time, the BHT of the injection well decreases and the cooling effect penetrates further toward the production well until the fluid reaching the production well has a temperature less than the initial reservoir temperature, i.e. thermal breakthrough occurs. After 30 years, the end point on this streamline produces the lowest temperature of all streamlines near the production well.

In the same way, the temperatures for the points on other streamlines are obtained. Of course, it will take a longer time for the fluid to reach the production well and the fluid temperature is higher, even as much as the rock temperature. It should be noted that the streamline starting in the negative x-axis direction will never reach the production well due to axisymmetry, and thus does not have any effect on the BHT of the production well. The temperature contours at time=1, 10 and 30 years for the fluid are shown in Figure 6. It can be seen clearly that with increasing time, the cooling effect penetrates farther away from the injection well.

Figure 7 also shows the thermal responses of the BHT of the production well or the outlet of the fractured reservoir for different flow rates.

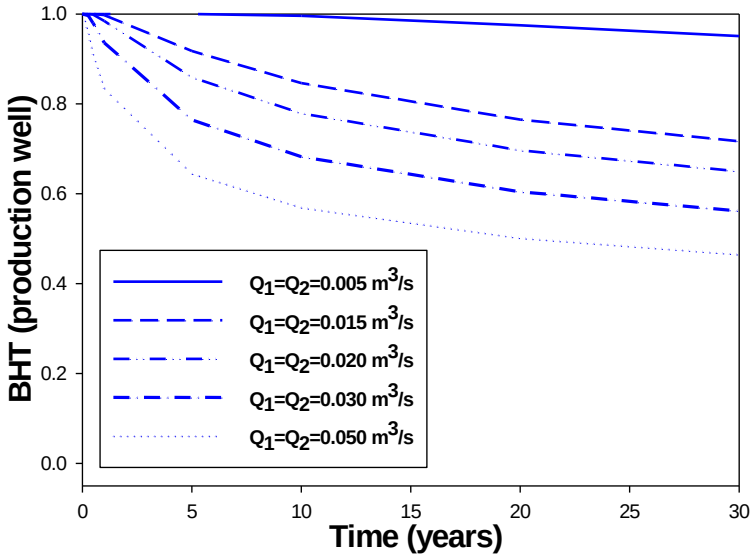

Figure 7: Dimensionless BHT of the production well under different flow rates when μ=5×10^{-4} Pa•s and 2L=500 m.

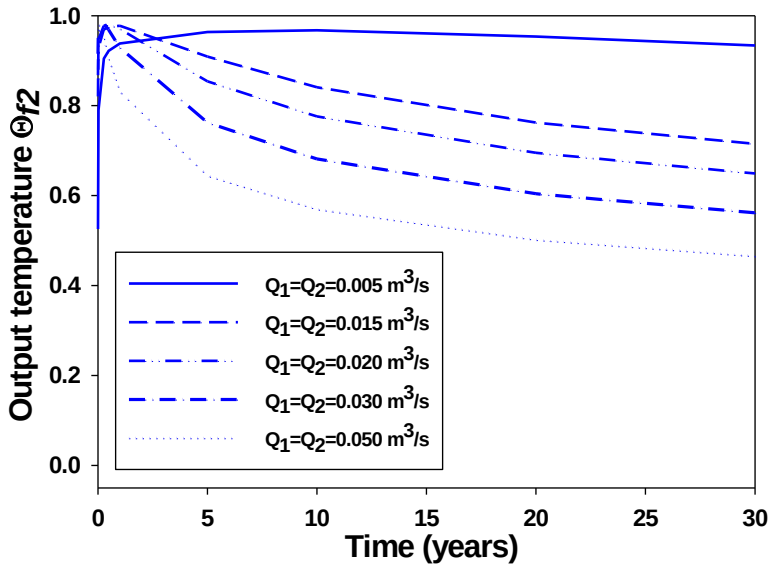

Figure 8: Dimensionless output temperature of the EGR system under different flow rates when μ=5×10^{-4} Pa•s and 2L=500 m.

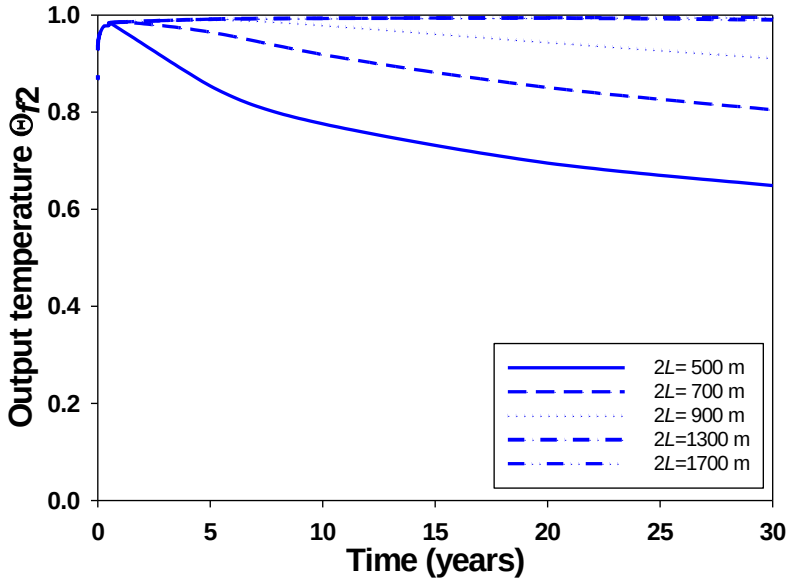

Figure 9: Dimensionless output temperature of the EGR system vs. Well distance when Q_1=Q_2=0.02 m^3 and μ=5×10^{-4} Pa•s.

(c) Thermal responses in the production well

One of the most important results is the final output temperature of the EGR. Although the water releases heat into the surrounding formation along the production well, the advection dominates the heat diffusion process and increases the fluid temperature in the upper part of the well. This can explains why the output temperature increases during the initial stage as shown Figure 8. With increasing time, the BHT decreases to be lower than the temperature at the upper part of the well, the output temperature will decrease after it reaches a maximum as shown in Figure 8. The time duration for the output temperature to reach its maximum is very short and is determined by the flow rate. By comparing Figures 7 and 8 we find that the BHT of the production well and the final output temperature show similar trends after several years, for the same reason that the BHT in the injection well eventually is equal to the surface injection temperature. At early time, their difference is still obvious. This means that the previous models, which assume the BHT of the production well to be the output temperature of the EGR system, are correct only for long production time conditions.

Another important factor which may affect the EGR productivity is the well separation. Figure 9 plots the output temperatures of the EGR vs. well distances. It is easy to understand that with other conditions remaining the same, a larger well separation increases the heat exchange time between the fluid in fracture and the surrounding high temperature rock, and thus produces a higher output temperature.

(d) Maximization of the output power of the EGR

Generally the output power of an EGR is expressed as in terms of $P= \rho_f c_f Q(T_{out}-T_{in})$. From Figure 8 we know that using higher flow rates produces lower output temperatures sooner. This indicates that larger flow rates do not necessarily produce higher output power. Therefore, there exist optimal values for these factors which maximize the output power of the EGR.

7. CONCLUSION

The closed-loop circulation in an EGR system is studied in this paper. After using some assumptions, the whole circulation is divided into three portions which can be solved independently based on the input conditions. A few conclusions can be made based on these numerical results:

(a) The great advantage of the present model is that the analytical solutions are obtained in the Laplace space and the model can be run in only a few seconds using a notebook computer. It is more efficient in time compared with other numerical methods such as FEM and BEM and this allows for numerous optimization runs;

(b) The assumptions used in this paper do not impact on the use or accuracy of the numerical results . The results can provide a basis for the EGR optimization and design;

(c) As the fluid viscosity does not affect greatly the BHT of the injection well, assuming the viscosity is constant does not significantly affect this calculation.

(d) The flow rates play an important role in the heat exchange in the wells and the fracture reservoir. The effect of rate vary with the well distance. An optimal choice of these factors requires more study;

(e) In addition, the validation against some field data of the present model is needed.

ACKNOWLEDGEMENTS

This work presented in this paper was supported by VEGAS Project, CSIRO Earth Science and Resource Engineering, Australia.

REFERENCES

Bödvarsson, G.S. 1969. On the temperature of water flowing through fractures. Journal of Geophysical Research. 74(8), 1987-1992.

Budd, A.R., Holgate, F.L., Gerner, E., Ayling, B.F. and Barnicoat, A., 2008. Pre-competitive geoscience for geothermal exploration and development in Australia: Geoscience Australia's onshore energy security program and the geothermal energy project, Australian Geothermal Energy Conference. 19-22 August, Melbourne, Australia.

Cheng A.H.D., Ghassemi, A., Detournay, E. 2001. Integral equation solution of heat extraction from a fracture in hot dry rock. International Journal for Numerical and Analytical Method in Geomechanics. 25, 1327.

DaCosta, J.A., Bennett, R.R. 1960. The pattern of flow in the vicinity of a recharging and discharging pair of wells in an aquifer having areal parallel flow. International Association of Scientific Hydrology. 52, 524-536.

Fomin, S., Hashida, T., Chugunov, V., Kuznetsov, A.V. 2005. A borehole temperature during drilling in a fractured rock formation.

International Journal of Heat and Mass Transfer. 48, 385–394.

Gnielinski, V.1976. New equations for heat and mass transfer in turbulent pipe and channel flow. International Chemical Engineering. 16(2), 359-368.

Ghassemi, A., Tarasovs, S., Cheng A.H.D. 2003. An integral equation solution for three-dimensional heat extraction from planar fracture in hot dry rock. International Journal for numerical and Analytical Methods in Geomechanics. 27, 989–1004.

Gradshteyn, I.S., and Ryzhik, I.M. 2007. Tables of integrals, series, and products. 7th edition, Academic Press.

Gringarten, A.C., Witherspoon, P.A., Ohnishi, Y. 1975.Theory of heat extraction from fractured hot dry rock. Journal of Geophysical Research. 80(8), 1975, 1120-1124.

Gringarten, A. C., Sauty, J. P. 1975. A theoretical study of heat extraction from aquifers with uniform regional flow. Journal of Geophysical Research. 80(35), 4956-4962.

Grove, D.B., Beetem, W.A., Sower F.B. 1970. Fluid travel time between a recharging and discharging well pair in an aquifer having a uniform regional flow field. Water Resources Research. 6(5), 1404-1410.

Heuer N., Kopper, T., Windelberg, D. 1991. Mathematical model of a hot dry rock system. Geophysical Journal International. 105, 659-664.

Holmes, C.S., Swift, S.C. 1970. Calculation of circulating mud temperatures. Journal of Petroleum Technology, 670-674.

Jiji, L.M.. 2009. Heat Conduction. Third edition. Springer-Verlag Berlin Heidelberg.

Keller, H.H., Couch, E.J., Berry, P.M. 1973. Temperature distribution in circulating mud columns. Old SPE Journal. 23-30.

Kolditz O. 1995. Modelling flow and heat transfer in fractured rocks: Conceptual model of a 3-D deterministic fracture network. Geothermics, 24(3), 421-437.

Lauwerier, H.A. 1995. The transport of heat in an oil layer caused by the injection of hot fluid. Applied Scientific Research. 5, 145-150.

Ogino,F., Yamamura, M., Fukuda, T. 1999. Heat transfer from hot dry rock to water flowing through a circular fracture. Geothermics. 28, 21-44

Rodemann, H. 1982. Analytical model calculations on heat exchange in a fracture. Urach Geothermal Project, Haenel R.(ed.), Stuttgart, 1982.

Ramey, H.J. 1962. Wellbore heat transmission. Journal of Petroleum Technology. 427–435.

Raymond, L.R. 1969. Temperature distribution in a circulating drilling fluid. SPE-AIME. 333-342.

Schulz, R. 1997. Analytical model calculations for heat exchange in a confined aquifer. Geophysical Journal International. 61, 12-20.

Stehfest, H. 1970. Algorithm 368: Numerical inversion of Laplace transforms. Communications of the ACM. 13, 47-49.

Sump, G.D., Williams, B.B. 1973. Prediction of wellbore temperature during mud circulation and cementing operations. Journal of Engineering for Industry, 1083-1092.

Willhite, G.P. 1967. Over-all heat transfer coefficients in steam and hot water injection wells. Journal of Petroleum Technology. 607-615.

Wooley, G.R. 1980. Computing dowhole temperatures in circulation, injection and production wells. Journal of Petroleum Technology, 1509-1522.

Wu, B., Zhang, X., Bunger, A. and Jeffrey, R. 2013a. An efficient and accurate approach for studying the heat extraction from multiple recharge and discharge wells. The International Conference for Effective and Sustainable Hydraulic Fracturing, 20-22 May 2013, Australia.

Wu, B., Zhang, X., Jeffrey, R. 2013b. A model for downhole fluid and rock temperature prediction during circulation. Submitted to Geothermics. In press, http://dx.doi.org/10.1016/j.geothermics.2013.10.004.

Yang, S., Yeh, H.. 2009. Modeling heat extraction from hot dry rock in a multi-well system. Applied Thermal Engineering. 29 1676–1681.